CRISPR/Cas9 gene editing for the creation of an MGAT1 deficient CHO cell line to control HIV-1 vaccine glycosylation

High mannose CHO line improves gp120 binding to antibodies

Authors: Gabriel Byrne[1], Sara M. O'Rourke[1], David L. Alexander[1], Bin Yu[1], Rachel C. Doran[1], Meredith Wright[1], Qiushi Chen[2], Parastoo Azadi[2], and Phillip W. Berman[1]

Affiliations: [1]Department of Biomolecular Engineering, University of California Santa Cruz, Santa Cruz, California United States of America. [2]Complex Carbohydrate Research Center, University of Georgia, Athens, Georgia, United States of America.

Keywords: HIV vaccine, glycosylation, CHO cells, neutralizing antibodies, gene editing, CRISPR/Cas9, gp120

Abstract

Over the last decade multiple broadly neutralizing monoclonal antibodies (bN-mAbs) to the HIV-1 envelope protein, gp120, have been described. Surprisingly many of these recognize epitopes consisting of both amino acid and glycan residues. Moreover, the glycans required for binding of these bN-mAbs are early intermediates in the N-linked glycosylation pathway. This type of glycosylation substantially alters the mass and net charge of HIV envelope (Env) proteins compared to molecules with the same amino acid sequence but possessing mature, complex (sialic acid containing) carbohydrates. Since cell lines suitable for biopharmaceutical production that limit N-linked glycosylation to mannose-5 (Man_5) or earlier intermediates are not readily available, the production of vaccine immunogens displaying these glycan dependent epitopes has been challenging. Here we report the development of a stable suspension adapted CHO cell line that limits glycosylation to Man_5 and earlier intermediates. This cell line was created using the CRISPR/Cas9 gene editing system and contains a mutation that inactivates the gene encoding Mannosyl (Alpha-1,3-)-Glycoprotein Beta-1,2-N-Acetylglucosaminyltransferase (MGAT1). Monomeric gp120s produced in the MGAT1$^-$ CHO cell line exhibit improved binding to prototypic glycan dependent bN-mAbs directed to the V1/V2 domain (e.g. PG9) and the V3 stem (e.g. PGT128 and 10-1074) while preserving the structure of the important glycan independent epitopes (e.g. VRC01). The ability of the MGAT1- CHO cell line to limit glycosylation to early intermediates in the N-linked glycosylation pathway, without impairing the doubling time

or ability to grow at high cell densities, suggest that it will be a useful substrate for the biopharmaceutical production of HIV-1 vaccine immunogens.

Introduction

Despite thirty years of research, a vaccine capable of providing protection against human immunodeficiency virus type 1 (HIV) has yet to be described. However, considerable progress towards this goal has been achieved with the elucidation of the 3-dimensional structure of the HIV-1 envelope proteins (monomeric gp120 and trimeric gp140) and the characterization of multiple broadly neutralizing monoclonal antibodies (bN-mAbs) (1-5). As headway toward a protective vaccine continues, the practicalities of large-scale vaccine production must be addressed. A growing body of evidence indicates that the N-linked glycosylation structure will be a critical factor in both the design and manufacture of any HIV vaccine (6-8).

Beginning in 2009, we learned that multiple bN-mAbs recognized glycan dependent epitopes on the HIV envelope protein, gp120. In an unanticipated development, several families of bN-mAbs require mannose-5 (Man_5) and/or mannose-9 (Man_9) for binding to key epitopes of gp120 (6, 9-11). As these bN-mAbs were being described, the data from the RV144 HIV vaccine trial was released. This study provided evidence for the first time that vaccination could prevent HIV infection in humans (12). The regimen used in this trial involved immunization with a bivalent gp120 vaccine (AIDSVAX B/E) to stimulate an antibody response as well as immunization with a recombinant canarypox vector to stimulate a cell mediated immune response (13-15). This immunization protocol resulted in modest (31.2%) but significant vaccine efficacy

(12). Examination of the gp120 subunit vaccines used in the RV144 trial showed that both components (MN-rgp120 and A244-rgp120) were enriched for complex, sialic acid containing glycans and lacked the high-mannose glycosylation found on the surface of virions and native envelope proteins required to bind the new class of glycan dependent bN-mAbs(16-20). Thus, differences in glycosylation between the vaccine immunogens from the RV144 trial and virus particles could, in part, explain the low efficacy of RV144 and other gp120 based vaccines and their inability to elicit broadly neutralizing antibodies (bN-mAbs). Previously we reported that the same gp120s used in the RV144 trial could be modified to bind multiple bN-mAbs when expressed in a cell line (HEK 293 GnTI$^-$) that limited N-linked glycosylation to Man_5, or earlier species (e.g. Man_8, Man_9) (21). While in theory this cell line could be used to produce a glycan optimized gp120 vaccine, in reality this is not practical. The HEK 293 GnTI$^-$ system is not suitable for clinical and large-scale production due to genetic instability and the inability to grow for sustained periods at high cell densities (22, 23).

CHO cells have long been the substrate of choice for the production of therapeutic glycoproteins. This is due to their ability to grow at high densities in serum-free suspension cultures, sustain high levels of protein expression over prolonged fermentation cycles, and incorporate complex glycans on exogenously expressed proteins (24-26). Typical glycoproteins contain only a few N-linked glycans, which aid in protein folding, intracellular trafficking. When these glycans terminate in sialic acid residues they increase resistance to proteolysis and extend serum half-life *in vivo* (27-29). Because of these physical and pharmacokinetic benefits, recombinant glycoprotein expression efforts have historically focused on maximizing the amount of complex, sialic

acid containing glycans per molecule. Although modern production technology provides the means to express and purify properly folded recombinant glycoproteins at large scale, controlling the glycosylation has been a persistent problem for most glycoproteins due to the "non-templated" nature of glycosylation (30-32). The final glycan structure of proteins with only a few N-linked glycosylation sites can be highly variable with respect to the glycan structure branching, saccharides present, sialic acid content, and net charge. Glycosylation heterogeneity is known to result from a variety of variables including: cell type, protein expression levels, cell culture conditions, monosaccharide donor availability, and protein structure (30, 33-36). Controlling glycosylation heterogeneity in gp120 is particularly problematic due to the fact that it contains an average of 25 potential N-linked glycosylation sites (PNGS), comprising approximately 50% of the mass of the mature protein (37-40). Each glycan site may be different in composition than others on the same molecule or different at the same position from molecule to molecule. Variance is so great that 79 different glycan structures have been found to occur a single position in envelope proteins expressed in normal CHO cells (41).

In this paper we address the problems of glycosylation heterogeneity and bN-mAb binding in the large-scale production of recombinant envelope proteins by the development of a mutant CHO cell line (MGAT1^{-} CHO) in which the Mannosyl (Alpha-1,3-)-Glycoprotein Beta-1,2-N-Acetylglucosaminyltransferase (MGAT1) gene has been inactivated using CRISPR/Cas9 gene editing. The nomenclature for MGAT1 gene has changed over the years and was previously referred to as the GnTI gene. Inactivation or deficiency of the MGAT1 limits N-linked glycosylation to early oligo-mannose glycans

(Man_{5-9}) and enhances the binding of bN-mAbs to glycans dependent epitopes, as compared to earlier gp120 vaccines produced in normal CHO cells. Although other CHO cell lines , such as CHO Lec1, have been described that similarly limit oligomannose-structures, they grow slowly, and differ from parental cell lines in morphology and growth characteristics (42, 43). Thus, the development of a precision-engineered CHO cell line resulting from by CRISPR/Cas9 gene editing, is a desirable alternative for HIV vaccine manufacturing. This cell line should be useful for the production of stable cell lines suitable for the production HIV vaccines as well as other biopharmaceuticals where limiting the incorporation of sialic acid is beneficial.

Results

Silencing of CHO-S MGAT1 Gene

The goal of this project was to make an MGAT1 deficient CHO-S cell line using CRIPSR/Cas9. With this gene knocked out, complex, sialic acid containing, glycans cannot be formed and N-linked glycosylation is not processed beyond the oligomannose Man_5 structure (Fig. 1). The CRISPR/Cas9 gene editing system allows for specific targeting of genes for deletion or modification by introducing double stranded breaks (DSB) followed by non-homologous end joining (NHEJ) or homology directed repair (HDR) (44, 45). We utilized a CRISPR/Cas9 nuclease vector containing an OFP reporter gene (Materials and Methods). After insertion of guide sequences, the vector

contained all of the elements needed to induce a double stranded break in the MGAT1 gene. The sequence of the CHO MGAT1 gene was identified from GenBank, gene ID: 100682529 (46). Three target specific double stranded guide sequences were ligated into the vector between a U6 promoter and a tracrRNA sequence. The same vector encodes the Cas9 endonuclease and an orange fluorescent protein reporter gene, separated by a self-cleaving 2A peptide linker. This system allows for a single plasmid to encode for both the Cas9 and a complete gRNA, enabling the use of non-Cas9 expressing cells. Following ligation of these guide sequences, the vectors were transfected into CHO-S cells using the MaxCyte electroporation system (Fig. 2). Targets 1 and 2 were introduced individually; target 3 plasmid was mixed and added together in equal ratio with target 2, creating three separate pools of transfected cells. Twenty-four hours post transfection samples were serially diluted across five 96 well flat-bottoms plates at a calculated density of 0.5 cells per well. The plates were examined daily, and wells with more than a single colony was discarded. Across the 15 total plates, between 15 and 30 wells per plate contained single viable colonies that were transferred to 24 well plates upon reaching 20% confluency after 12 to 15 days. Wells in the 96 well plates that did not have at least several dozen cells by day 15 were discarded. A total of 166 colonies were expanded to 24 well plates: 55 from target 1 pool, 67 from target 2 pool, and 44 from combined target 2/3 pool.

Fig 1. Simplified view of N-linked glycosylation pathway. N-linked glycosylation begins in the endoplasmic reticulum with the en-block transfer of a highly conserved $Glc_3Man_9GlcNAc_2$ structure (left) to asparagine residues within the N-X-S/T motif of

nascent proteins. This initial structure is sequentially trimmed to $Man_9GlcNAc_2$ and then $Man_5GlcNAc_2$ (center) as the protein moves from the ER to the Golgi apparatus. The enzyme, Mannosyl (Alpha-1,3-)-Glycoprotein (Beta-1,2)-N-Acetylglucosaminyl-transferase (MGAT1, red box) adds an N-acetylglucosamine to the Man_5 structure and is required to enable other glycosyltransferases to add monosaccharides creating hybrid (second from right) and complex (right) glycoforms. Treatment with endoglycosidase H (Endo H) cleaves simple, oligomannose containing glycans from glycoproteins, but not complex sialic acid containing glycans. PNGase F removes both simple and complex glycans from glycoproteins (indicated by the arrows). Kifunensine and swainsonine are inhibitors that halt processing at the steps indicated. Dashed black arrows indicate multiple enzymatic steps. Figure adapted from Binley, J.M., et al., *Role of Complex Carbohydrates in Human Immunodeficiency Virus Type 1 Infection and Resistance to Antibody Neutralization.* Journal of Virology, 2010. 84(11): p. 5637-5655. (47)

Fig 2. Flow chart of MGAT1 gene editing and cell line selection strategy. (A) A plasmid containing the Cas9 nuclease, tracrRNA, and a guide RNA (gRNA) sequence was electroporated into suspension adapted CHO-S cells. (B) Twenty-four hours following transfection, the cells were distributed into 96 well tissue culture plates at a density of 0.5 cells/well. (C) Between 12 and 15 days later, wells with 20% or greater confluency were transferred to 24 well plates. (D) After five days of growth in 24 well plates, a 0.2mL aliquot was removed from each well and cells were tested for the ability to bind fluorescein labeled Galanthus nivalis lectin (GNA). (E) GNA binding cells were

176 then expanded to shake flasks and cell lines were transiently transfected with a gene
177 encoding A244-rgp120. The cell culture supernatants were then collected after five days
178 and tested for binding of gp120 to the prototypic glycan dependent, broadly neutralizing
179 monoclonal antibody, PG9. (G) The gene encoding MGAT1 was sequenced from GNA
180 binding cell lines with that exhibited robust growth and the ability to secrete PG9 binding
181 gp120. The specific mutations induced by non-homologous end joining repair (NHEJR)
182 were determined by Sanger sequencing.

183

184 Lectin binding to detect MGAT1 gene inactivation

185 If the MGAT1 gene were inactivated, we expect glycoproteins to possess exclusively
186 oligo-mannose forms of N-linked glycosylation, with a preponderance of Man_5 isoforms
187 on cell surface and secreted proteins. The lectin GNA recognizes glycans with terminal
188 alpha-D mannose and is unable to bind to sialic acid containing complex glycans (48).
189 Accordingly we used fluorescein conjugated GNA to determine whether CRISPR/Cas9
190 transfected cells possessed a phenotype characteristic of cells with an inactivated
191 MGAT1 gene. GNA does not require Ca^{2+} or Mg^{2+} cofactors to bind, allowing the use of
192 10μM EDTA to ameliorate cell clumping during repeated centrifugation and wash steps.
193 While MGAT1^{-} CHO cells and control HEK 293 GnTI^{-} cells bound to the GNA lectin, the
194 wild type CHO-S cell line did not (Fig. 3). A total of 20 GNA binding cell lines from the
195 original 166 candidates were selected on the basis of uniform GNA binding and the
196 cultures were expanded for further analysis. Three days following initial GNA selection,

197 the 20 cell line candidates were re-examined and six were rejected for lack of uniform
198 lectin binding across the sample population, leaving 14 candidates.

199

200 **Fig 3. GNA lectin probe for cell surface oligomannose glycan expression.** The
201 GNA lectin binds glycan structures with terminal mannose and will not bind complex,
202 sialic acid containing glycans. CHO-S cells were transfected with a plasmid designed to
203 inactivate the MGAT1 gene by CRISPR/Cas9 gene editing (MGAT CHO). The cells
204 were treated with fluorescein conjugated GNA lectin to screen for the incorporation of
205 high mannose glycans in the cell membrane. HEK 293 GnTI$^-$ cells that also lack the
206 MGAT1 gene served as a positive control (panels A and D) while normal CHO-S cells
207 that possess an intact MGAT1 gene served as a negative control (panels B and E).
208 Cells were visualized under 20 x magnification on a Leica DM5500 B widefield
209 microscope using differential interference contrast (DIC) (upper panels A, B, C) or under
210 illumination with 495nm light (lower panels D, E, and F).

211

212 Expression of gp120 in MGAT1$^-$ CHO cell lines

213 Based on positive lectin binding criteria, the 14 candidate cell lines were grown in
214 125mL shake flasks (Fig. 2). Of those, the four fastest growing (3.4F10, 3.5D8, 3.5A2,
215 and 3.4D9) were utilized for transient transfection with a gene encoding gp120 from the
216 A244 strain of HIV-1 (A244-rgp120). Also transfected was the CHO-S parental cell line
217 for comparison. This gp120 A244 had the sequence point mutations E332N and N334S,

introducing a PNGS at N332. Five days post transfection the culture media was harvested and secreted gp120 proteins were purified by immunoaffinity chromatography. The purified products were assayed for protein yield, tested for identity using immunoblot analysis (data not shown) and for the ability to bind the glycan dependent bNAb, PG9 by fluorescent immune assay (FIA) (Fig. 4). Previous studies have shown that this bNAb requires Man_5 at position N160 in the V1/V2 domain for binding (3). The results from this study confirmed that the MGAT1$^-$ CHO cell lines could bind this antibody whereas gp120 produced in the parental CHO-S cell line was unable to bind PG9. From this analysis, a single MGAT1$^-$ CHO cell line, 3.4F10, was selected for further characterization and analysis (Fig. 4).

To be a viable substrate for biopharmaceutical production, the growth and protein yield of the knockout line had to be comparable to the parental line. In transient transfection experiments the calculated recovery of purified protein was 35.4mg/L for the 3.4F10 MGAT1$^-$ CHO line and 32.2mg/L for the parental CHO-S line. Production of the same protein in HEK 293 GnTI$^-$ cells by transient transfection yielded 1.9mg/L. We measured that the cell doubling time for the 3.4F10 MGAT1$^-$ CHO cell line in BalanCD CHO Growth A media was 20.7 hours in a 1L shaker flask during logarithmic growth phase, reaching a density of $1.9x10^7$ cells/mL. This was similar to the parental CHO-S population doubling time of 19.0 hours that achieved cell densities of $1.6x10^7$ cells/mL. By comparison, the GnTI$^-$ HEK 293 cell line had a logarithmic cell doubling time of 23.3 hrs. and achieved a maximal cell density of 4.20 $x10^6$ cells/mL when grown in Freestyle 293 media.

Fig 4. Screening and Sequence Analysis of MGAT1$^-$ CHO cell line: Colonies selected after MGAT1 gene inactivation were transiently transfected with a gene encoding A244-rgp120. Cell culture supernatants were collected and tested for binding by the glycan dependent bN-mAb PG9. Based on PG9 binding studies the MGAT genes from selected cell lines were amplified by PCR and sequenced. (A) PG9 binding to gp120 in cell culture supernatants of transiently transfected MGAT1$^-$ CHO lines 3.5D9, 3.5D8, 3.4F10, 3.5A2, and by supernatants from gp120 transfected CHO-S and GnTI$^-$ 293 HEK cells. (B) Diagram of the unaltered CHO-S MGAT1 gene target section with guide RNA (gRNA) complement sequence shown in blue and the protospacer adjacent motif (PAM) underlined in bold type. (C) Sequences of the MGAT1 gene for 3.4F10 and 3.5D8 cell lines both had the same single base insertion, shown in black box. (D) The sequence from the cell line 3.5A2 with bases deleted shown in box. (E) The bases deleted 3.5D9 cell line sequences are indicated by the box.

Identification of CRISPR/Cas9 induced genetic alteration

To confirm that MGAT1 gene had been inactivated, we sequenced the gene from the 3.4F10 line and the next three best candidates. An extra thymidine had been inserted at the Cas9 cleavage site of the 3.4F10 line MGAT1 gene, introducing a frame shift mutation. This mutation resulted in 23 altered codons and the insertion of a premature stop codon. The 3.5D8 line contained the same mutation, while 3.5D9 and 3.5A2 both had in frame deletions of 24 and 30 nucleotides respectively. The deleted codons of

3.5D9 and 3.5A2 corresponded to the transmembrane domain of the GnTI protein leaving the active extracellular domain intact. The diminished binding of gp120s produced in the 3.5D9 and 3.5 A2 clones to PG9 suggest that partial MGAT1 activity remains in these two clones compared to the 3.4F10 clone that, like gp120 produced in GnTI$^-$ cells, exhibits improved binding to PG9 (Figure 4). Given that the single base insertion in the 3.4F10 MGAT1 gene resulted in a frame shift 51 nucleotides into a 1276bp long gene, it is highly unlikely that the function of this gene could be restored by random mutation.

Characterization of MGAT1$^-$ CHO gp120 glycosylation

Two additional methods (endoglycosidase digestion and mass spectrometry analysis using MALDI-TOF-MS) were used to further characterize the N-linked glycosylation incorporated in A244-rgp120 produced by the 3.4F10 MGAT1$^-$ CHO cell line. Immunoaffinity purified, monomeric A244 gp120 produced by the CHO-S, HEK 293 GnTI$^-$, and MGAT1$^-$ CHO cell lines were digested overnight by endoglycosidases PNGase F and Endo H, then analyzed by SDS-PAGE and stained with Coomassie blue dye (Fig. 5). Endo H cleaves N-linked high-mannose glycan structures, and not complex, sialic acid containing glycans. When the protein produced in the HEK 293 GnTI$^-$ and MGAT1$^-$ CHO cell lines was compared to the proteins produced in CHO-S cell lines, we noted a reduction in mass of approximately 20kD. This is in keeping with the smaller mass of the Man_5 glycoform compared to that of the hybrid and complex glycans found on CHO-S produced material. Following Endo H digestion, the protein

produced in the CHO-S cell line was largely unaltered, indicating that it possessed the normal complex, sialic acid containing glycans. In contrast, the proteins produced in the MGAT1$^-$ CHO and HEK 293 GnTI$^-$ cells were reduced to ~60kD in size. This result was consistent with the observation that approximately half the mass of a given gp120 molecule can be attributed to N-linked glycosylation (47, 49, 50). The complete sensitivity of the proteins produced in the MGAT1$^-$ CHO and HEK 293 GnTI$^-$ cells to Endo H digestion suggests that the glycosylation of these cell lines is exclusively high-mannose. When digested with PNGase F, all samples dropped to the same size, confirming that undigested gp120 size variances were due to glycosylation differences.

Fig 5. Endoglycosidase analysis of gp120 produced in MGAT1$^-$ CHO cell line. Purified A244 rgp120 recovered from transiently transfected CHO-S, MGAT1$^-$ CHO, or HEK 293 GnTI$^-$ cell lines was analyzed by SDS-PAGE following endoglycosidase treatment. Purified gp120s were reduced and denatured then treated with either endoglycosidase H (Endo H) or Peptide:N-Glycosidase F (PNGase F). The digests were then analyzed on 4-12% tris-glycine SDS PAGE gels and stained with Coomasie blue dye. Panel A, mock digests of gp120s produced in CHO-S, MGAT1$^-$ CHO, and HEK 293 GnTI$^-$ cells. Panel B, the same proteins in panel A, digested with endoglycosidase H (Endo H). Panel C, the same proteins in panel A, digested with PNGase F. The mobility of molecular weight markers is shown for each gel. The endoglycosidases proteins are visible as bands at 29kD (Endo H, panel B) and 36kD (PNGase F, panel C).

Additional studies were carried out to characterize the specific glycans incorporated in the A244-rgp120 produced in the MGAT1$^-$ CHO and the CHO-S cell lines. Using MALDI-TOF-MS (Fig. 6), we found that 56.4% of the N-linked glycans present on the MGAT1$^-$ CHO produced gp120 were Man_5, 19.2% were Man_9, 11% were Man_8 and the remainder were Man_6 and Man_7. No complex sialic acid containing glycans were detected (Table 1). The degree of fucosylation was also significantly lowered; fucosylation was only on Man_5 glycoforms at the core GlcNAc and represented 3.16% of the total glycans present.

When the A244-rgp120 produced in CHO-S cells was examined, approximately 75% of the glycans were complex or hybrid glycans and 25% represented the early intermediates ranging from Man_5 to Man_9. No high mannose species were detected with core GlcNAc fucose attached, but nearly all hybrid and complex glycans were fucosylated.

Fig 6. MALDI-TOF analysis of glycans present on gp120 produced by CHO-S and MGAT1$^-$ CHO cell lines. The carbohydrates on purified A244 gp120s produced by CHO-S (A) and MGAT1$^-$ CHO (B) cells were released by PNGase F digestion and examined by MALDI-TOF MS as described in Materials and Methods. Pie charts indicate the percentage of high-mannose (blue), complex (red), and potential bisected

(green) N-linked glycans. This analysis was performed by the Complex Carbohydrate Research Center at the University of Georgia.

Table 1. Percentage of different glycan species on gp120 produced by CHO-S and MGAT1$^-$ CHO cells.

	Cell Line	
Glycan Species	CHO-S	MGAT1$^-$ CHO
Man_5	5.2%	56.4%
Man_6	1.9%	4.5%
Man_7	3.3%	7.1%
Man_8	5.1%	11.4%
Man_9	9.6%	19.2%
Complex or Hybrid	75%	0.53%

Percentages calculated from MALDI-TOF peak intensity.

Binding multiple bN-mAbs to gp120 expressed in the MGAT1$^-$ CHO cells.

We next compared A244-rgp120 expressed in the MGAT1$^-$ CHO cells with A244-rgp120 produced in normal CHO-S cells for the ability to bind bN-mAbs in a FIA. A panel of prototypic bN-mAbs that recognize distinct sites of virus vulnerability in monomeric and trimeric HIV envelope proteins were utilized (Fig. 7). We noted a significant improvement in the binding of PG9, CH01 and CH03 to the proteins expressed in MGAT1$^-$ CHO cells and HEK 293 GnTI$^-$ cells compared to the CHO-S cells. These bN-mAbs are known to bind to epitopes in the V1/V2 domain that require Man_5 at the N160 glycosylation site (3). Similarly we noted a significant improvement in

346 the binding of the PGT126 and PGT128 bN-mAbs that require oligo-mannose glycans
347 at the N301 and N332 glycosylation sites in the stem of the V3 domain (51). Mixed
348 results were seen for the PGT121 family of bN-mAbs where the binding to gp120
349 produced in both the MGAT1$^-$ CHO and HEK 293 GnTI$^-$ cells lines was lower than
350 binding of these antibodies to gp120 produced in the CHO-S cell line. In contrast,
351 binding to the 10-1074 bN-mAb, also in the PGT121 family, was unaffected by the
352 cellular substrate used for production. These results demonstrate that changing the
353 glycosylation, while leaving the amino acid sequence intact can significantly improve the
354 antigenic structure of A244-rgp120 with respect to the binding of several bNAbs to
355 glycan dependent epitopes. The effect of differences in glycosylation was also
356 examined on the binding of the VRC01 bN-mAb, known to recognize a glycan
357 independent epitope adjacent to the CD4 binding site (52). While this antibody bound to
358 all of the envelope proteins tested, a small, but consistent improvement in binding was
359 observed to the proteins produced in the MGAT1$^-$ CHO and HEK 293 GnTI$^-$ cells
360 compared to the protein produced in the CHO-S cells. These studies suggest that the
361 sialic acid containing hybrid and complex carbohydrates incorporated in normal cell
362 lines in some way interfere with the VRC01 binding site on monomeric gp120. This
363 same effect may be observed with further non-glycan dependent antibodies by
364 decreasing the glycan interference.
365
366 **Fig 7. Comparison of bN-mAb binding to A244-rgp120 produced in MGAT1$^-$ CHO**
367 **cells, CHO-S cells and HEK 293 GnTI$^-$ cells.** The binding of a panel of broadly
368 neutralizing monoclonal antibodies to purified A244-rgp120 produced in MGAT1$^-$ CHO

cells, CHO-S cells, and HEK 293 GnTI$^-$ cells was measured in a Fluorescence Immunoassay (FIA). Briefly, purified proteins were captured onto wells of black 96 well microtiter plates coated with a mouse monoclonal antibody against the N-terminal gD tag present in all three proteins. Plates were then incubated with serial dilutions of bN-mAbs targeting: glycan-epitopes within the V1V2 domain (PG9, CHO1 and CHO3), the glycan-epitopes within the V3 domain (PGT128, PGT126, PGT121, 10-1074 and PGT122), or the CD4 binding site (VRC01). Plates were incubated with a 1:3,000 dilution of AlexaFluor 488 conjugated goat-anti-human polyclonal antibody and binding is reported as Relative Fluorescence Units (RFU). FIA details are provided in Materials and Methods.

MVM infectivity

Minute virus of mice (MVM) is a small inactivation resistant virus that is ubiquitous in the environment and a major cause of bioreactor culture failure in biopharmaceutical manufacturing (53). As sialic acid is a major receptor for MVM infectivity, the MGAT1$^-$ CHO cell line we created might have the additional manufacturing benefit of being resistant to MVM infection (54). To investigate this possibility, the MGAT1$^-$ CHO cell line was tested for infectivity resistance to two strains of MVM using a qPCR assay and compared to wild type CHO-S MVM sensitivity. While the MGAT1$^-$ CHO cell line was similarly sensitive to the MVMp strain as wild type CHO-S cells, it was resistant to MVMc infection (Table 2). The receptor protein for MVM have not yet been identified, but it has been demonstrated that MVMp binds to sialic acid residues from both N and

O linked glycosylation (55-57). Knocking out MGAT1 does not alter the O-linked glycosylation pathway, perhaps explaining why the line remains sensitive to MVMp. MVMc is a more recently identified strain(58) with little information available on its binding to CHO or murine cells. Anything beyond noting the apparent dependence on complex N-linked glycosylation would be speculative at this point.

Table 2: MVM infectivity assay

MVM type	Cell	MVM Cp	18s Cp	MVM Copies	18S Copies	MVM/18S	MVM/18S
MVMp	CHO-S	5.80	17.98	2.23E+10	2.03E+06	1.13E+04	1.13E+04
	MGAT1$^-$ CHO	6.11	18.74	1.95E+10	1.22E+06	1.49E+04	1.49E+04
MVMc	CHO-S	7.91	18.91	5.04E+09	1.07E+06	4.84E+03	4.84E+03
	MGAT1$^-$ CHO	19.3	19.6	2.00E+06	6.91E+05	2.92E+00	2.92E+00

MVMp, minute virus of mice prototypic strain; MVMc, minute virus of mice Cutter strain; Cp, QPCR crossover point, the cycle at which fluorescence from amplification becomes greater than background, used to infer copy number against a standard curve with a lower Cp; 18S, eukaryotic ribosomal subunit. All values are the mean of a triplicate set.

This infectivity assay was performed by IDEXX BioResearch (Columbia, MO).

Adventitious agent testing

The cell line was tested for the presence of mycoplasma, cross-species contamination, and viral contaminants by IDEXX BioResearch (Columbia, MO). No adventitious agents were detected. The full list and procedure are described in the supplemental materials.

Discussion

A major goal in HIV vaccine research is to develop immunogens that elicit bNAbs. The discovery that multiple bN-mAbs to HIV recognize glycan dependent epitopes has altered our thinking of how best to produce this vaccine. Instead of using standard CHO cell production cell lines, that incorporate complex and hybrid glycosylation, a cell line that limits glycosylation to high-mannose forms may be useful for gp120 immunogens. While we have long been able to produce properly folded Env protein monomers (gp120 and gp140) as indicated by the ability to bind CD4 with high affinity (59-63), until now we have not been able to replicate the glycan structures required for the binding of multiple families of bN-mAbs in expression systems suitable for large scale manufacturing.

The glycans that decorate the surface of native, virion-associated, HIV Env protein are typically enriched for high-mannose variants, normally found on early intermediate proteins within the ER and early Golgi (18, 19). This unusual restriction in glycan maturation is thought to be a consequence of steric hindrance occurring during the formation of trimeric virus spike structures (64). Additionally, the high density of PNGS that likely evolved as a glycan shield to prevent immune recognition of virus sequences (38, 47, 65) appears to limit glycosidase and glycosyltransferase modifications of Env glycans in the late ER and early Golgi Apparatus (GA) (18, 64). While expression of monomeric gp120 results in incorporation of complex glycosylation, trimeric spike formation results in incomplete glycosylation and enrichment of virions with high-mannose glycans (18, 19). These differences in glycosylation might explain the inability of previous HIV vaccines to elicit bNAbs to glycan dependent epitopes in

humans. However they don't explain the inability of previous vaccines to elicit bNAbs to epitopes such as VRC01 that were present in most gp120 vaccines expressed in normal CHO cells. Earlier vaccines such as the AIDSVAX B/E used in the RV144 trial largely possessed complex sialic acid containing glycans and lacked the high-mannose glycans required for a variety of bN-mAbs including PG9, CH01, CH03, PGT128, and 10-1074 (16). Although the level of protection achieved in the 16,000-person RV144 trial was statistically significant (31.2%, P=0.04) this level was not sufficient for product registration or clinical deployment. In this regard, the addition of one or more epitopes recognized by bN-mAbs, such as the PG9 and PGT128 epitopes described in this report, might improve the antigenic structure and immunogenicity of or recombinant gp120 such that a level of protection of 50% or more, required for product approval is achieved. Currently RV144 follow-up studies are in progress that make use of sialic acid containing gp120 vaccine antigens, produced in normal CHO cells, like those used in the original RV144 trial (66, 67). These new trials are trying to improve the level of vaccine efficacy by prolonging the immunization schedule, altering the adjuvant formulation, and replacing the canarypox vector co-administered with gp120 with stronger, more virulent virus vectors.

Few methods currently exist to produce recombinant proteins incorporating the Man_5 and Man_9 glycans that are present in the HIV gp120 envelope protein. Expression of gp120 in yeast results in the incorporation of long chain high-mannose glycans (68), and insect expression systems produce a preponderance of paucimannose forms (Man_{3-4}) (69). Glycosidase inhibitors (e.g. kifunensine and swainsonine, see Fig. 1) are effective and useful for producing analytical quantities of proteins with Man_5 and Man_9

intermediates, but are highly toxic and prohibitively expensive for large-scale biopharmaceutical production (70, 71). Additionally, there exists evidence to suggest a broad mannosidase inhibitor like kifunensine may negatively impact protein folding through interference of the Calnexin/Calreticulin pathway (72-75). Glycosaminyl-transferase knockout cell lines from 293 HEK and CHO cells, referred to as HEK 293 GnTI$^-$ and CHO Lec1, respectively, have previously been described. They were generated through random ethyl methanesulfonate (EMS) mutagenesis, zinc finger methods, or screened for modified glycosylation by resistance to cytotoxic lectin binding (76-78). These lines lack a functional MGAT1 gene, responsible for the protein GnTI. Knocking out the MGAT1 gene prevents processing of glycans beyond the $Man_5GlcNAc_2$ stage, resulting in exclusively high-mannose glycoprotein production (28, 29). Such cell lines do not generally grow as robustly as their parental counterparts and raise potential regulatory issues with potential uncharacterized genetic alterations. In light of this, there is an unmet need for a cell line suitable for the scalable production of HIV vaccine immunogens. We have addressed this problem by creating the novel MGAT1$^-$ CHO cell line described above. Our data suggests that this cell line possesses several essential characteristics required for current Good Manufacturing Practices (cGMP) such as robust growth in well defined serum free medium, the ability to grow to high cell densities in suspension culture, a well defined mutation of the MGAT1 gene, and freedom from contamination by adventitious agents. However, the ultimate utility of this cell line will require characterization of stable cell lines with transfected envelope proteins where the genetic stability of the transgene as well as the quality and yield of the final product is determined.

Recombinant envelope proteins produced in the MGAT1$^-$ CHO cell line, such as the A244-rgp120 described in this report, can be used to test the hypothesis that previous HIV vaccines such as the AIDSVAX B/E vaccine used in the RV144 trial (12-14) were ineffective because they lacked the glycan dependent epitopes required to stimulate the formation of bN-mAbs. While the CHO MGAT1$^-$ cell line provides a practical way to produce envelope proteins with several glycan dependent epitopes recognized by bNAbs not present on gp120s produced in normal CHO cell lines, we do not yet know whether these epitopes will be immunogenic. Previous gp120 vaccine trials such as RV144 failed to detect glycan independent VRC01-like antibodies even though the VRC01 epitope was present on at least two different gp120s used for immunization. Thus, some epitopes recognized by bNAbs are poorly immunogenic and additional immunogenicity and formulation studies will likely be required to optimize virus neutralizing antibody responses to the glycan epitopes of the type described in this paper. Although the gp120 expression data presented here was derived exclusively from small-scale transient transfection experiments, we anticipate that the cell line described in this report will be useful for the development of stable MGAT1$^-$ CHO cell lines producing vaccines based on a variety of new concepts. These include guided immunization to stimulate germline genes encoding bNAbs (79-81), Env proteins designed with features that enhance antigen processing and presentation (82) as well as glycopeptide scaffolds that enhance the immunogenicity of epitopes recognized by bN-mAbs while eliminating non-protective immunodominant epitopes (21).

Materials and methods

Cell culture

Suspension adapted CHO-S cells were obtained from Thermo Fisher (Thermo Fisher, Life Technologies, Carlsbad, CA). HEK 293 GnTI$^-$ suspension adapted cells were obtained from ATCC (ATCC, Manassas, VA). Stocks of suspension adapted CHO-S and HEK 293 GnTI$^-$ cells were maintained in shake flasks (Corning, Corning, NY) using a Kuhner ISF1-X shaker incubator (Kuhner, Birsfelden, Switzerland). For cell propagation, shake flask cultures were maintained at 37°C, 8% CO_2, and 125 rpm. Static cultures were maintained in 96 or 24 well cell culture dishes and grown in a Sanyo incubator (Sanyo, Moriguchi, Osaka, Japan) at 37°C and 8% CO_2.

CHO-S cells were maintained in CD-CHO medium supplemented with 0.1% pluronic acid, 8mM GlutaMax and 1X Hypoxanthine/Thymidine (Thermo Fisher, Life Technologies, Carlsbad, CA). For cell growth studies, CHO cells were grown in BalanCD CHO Growth A Medium (Irving Scientific, Santa Ana, CA). HEK 293 GnTI$^-$ cells were maintained in Freestyle 293 cell culture media (Life Technologies, Carlsbad, CA). During transient CHO cell protein production the cells were maintained in OptiCHO medium supplemented with 0.1% pluronic acid, 2mM GlutaMax and 1X H/T (Thermo Fisher, Life Technologies, Carlsbad, CA). For protein production experiments the growth medium was supplemented with CHO Growth A (Molecular Devices, Sunnyvale, CA), 0.5% Yeastolate (BD, Franklin Lakes, NJ), 2.5% CHO-CD Efficient Feed A; and 0.25mM GlutaMax, 2 g/L Glucose (Sigma-Aldrich St. Louis, MO). Cell counts were performed using a TC20^{TM} automated cell counter (BioRad, Hercules, CA) with viability determined by trypan blue (Thermo Fisher, Life Technologies, Carlsbad, CA) exclusion.

Cell-doubling time in hours was calculated using the formula: $((T_2-T_1) \times \log_2) / (\log(D_2)-\log(D_1))$, where T = time at count and D = density at count. Cell count numbers used for doubling time calculation were from the logarithmic phase of growth.

Gene sequencing

The sequence of the MGAT1 CHO gene was confirmed using primers based on the predicted mRNA transcript (XM_007644560.1 (83)). Genomic DNA was extracted using the AllPrep kit (Qiagen, Germantown, MD). The MGAT1 gene was PCR amplified using the primers F_CAGGCAAGCCAAAGGCAGCCTTG and R_CTCAGGGACTGCAGGCCTGTCTC (Eurofins Genomics, Louisville, KY) with Taq and dNTPs supplied by New England BioLabs (Ipswich, MA). The PCR product was gel purified using a Zymoclean kit (Zymo Research, Irvine, CA), then sequenced by Sanger method at the (UC Berkeley, Berkeley, CA). MGAT1 knockouts were sequenced in the same manner.

CRISPR/Cas9 target design and plasmid preparation

We utilized a CRISPR/Cas9 nuclease vector with an OFP reporter (GeneArt, Thermo Fischer Scientific, Waltham, MA). Three target sequences to knock out the CHO-S MGAT1 gene were designed using an online CRISPR RNA Configurator tool (GE Dharmacon, Lafayette, CO). Target 1: CCCTGGAACTTGCGGTGGTC.Target 2: GGGCATTCCAGCCCACAAAG. Target 3: GGCGGAACACCTCACGGGTG. Each sequence was run in NCBI's BLAST tool for homologies with off-target sites in the CHO genome. Single stranded DNA oligonucleotides and their complement strands were synthesized (Eurofins Genomics, Louisville, KY) with extra bases on the 3' ends for ligation into GeneArt CRISPR nuclease vector (Thermo Fisher, GeneArt, Waltham, MA).

The strands were ligated and annealed into a GeneArt CRISPR vector using the protocol and reagents supplied with the kit. One Shot® TOP10 Chemically Competent *E. coli* were transformed and plated following the Invitrogen protocol (Thermo Fisher, Invitrogen, Carlsbad, CA). These were incubated in 5mL LB broth at 37°C in a shaking incubator at 225rpm overnight. Minipreps were performed according to manufactures instructions (Qiagen, Germantown, MD) and sent to UC Berkeley DNA Sequencing Facility (Berkeley, CA) with the U6 primers included in the GeneArt® CRISPR kit to confirm successful integration of guide sequences. A single 500mL Maxiprep was performed for each of the three target sequences using PureLink^{tm} Maxiprep kit (Thermo Fisher, Invitrogen, Carlsbad, CA).

Electroporation

Electroporation of CHO cells was performed using a MaxCyte STX scalable transfection system (MaxCyte Inc., Gaithersburg, MD) according to the manufacturer's instructions. Briefly, CHO-S cells were maintained at >95% viability prior to transfection. Cells were pelleted at 250g for 10 minutes, and then re-suspended in MaxCyte EP buffer (MaxCyte Inc., Gaithersburg, MD) at a density of $2x10^8$ cells/mL. Transfections were carried out in the OC-400 processing assembly (MaxCyte Inc., Gaithersburg, MD) with a total volume of 400μL and $8x10^7$ total cells. CRISPR/Cas9 exonuclease with guide sequence plasmid DNA suspended in endotoxin-free water was added to the cells in EP buffer for a final concentration of 300μg of DNA/mL. The processing assemblies were then transferred to the MaxCyte STX electroporation device and CHO protocol was selected using the MaxCyte STX software. Following electroporation, the cells in electroporation buffer were removed from the processing assembly and placed in

125mL Erlenmeyer cell culture shake flasks (Corning, Corning, NY). The flasks were placed into 37°C incubators with no agitation for 40 minutes. Following the rest period pre-warmed OPTI-CHO media was added to the flasks for a final cell density of $4x10^6$ cells/mL. Flasks were then moved to a Kuhner shaker and agitated at 125rpm.

Plating, expansion, and culture of CRISPR transfected CHO-S cells

Twenty-four hours post transfection a 100µL aliquot was taken from each of the transfected pools to assay for cell viability and orange fluorescent protein (OFP) expression using a light microscope (Zeiss Axioskop 2, Zeiss, Jena, Germany). Ninety-six well flat bottom cell culture plates (Corning, Corning, NY) were filled with 50µL of conditioned CD-CHO media. Each of the three transfected pools were serially diluted with warmed media to 10 cells/mL and added to five plates per pool in 50µL volumes. Final calculated cell density was 0.5 cells/well in 100µL of media. Once any single-colony well reached ≈20% confluency, the contents were transferred to a 24 well cell culture plate (Corning, Corning, NY) with 500uL of fresh media. When confluency reached 50%, a 200µL aliquot was removed for testing via a GNA lectin-binding assay. Following positive lectin binding, cells were moved to a 6 well cell culture plate (Corning, Corning, NY) with 2mL of media per well. After 5 days of growth in 6 well plates the GNA assay was repeated. Colonies exhibiting positive lectin binding were moved to 125mL shake flasks with an initial 6mL of media. Daily counts were taken and cell cultures expanded to maintain $0.3x10^6$ - $1.0x10^6$ cells/mL density.

Lectin binding assay

Fluorescein labeled *Galanthus nivalis* lectin (GNA), from the snowdrop pea (Vector Laboratories, Burlingame, CA), was used to detect the cell surface expression of Man_5 glycoforms. Cell aliquots (200µL) from 24 well plates were pelleted at 3000 rpm for three minutes. The supernatant was discarded and the cell pellet washed three times with 500µL of ice-cold 10µM EDTA in (Boston BioProducts, Ashland, MA) phosphate buffered saline (PBS) (Thermo Fisher, Gibco, Carlsbad, CA). The cell pellet was then re-suspended in 200µL ice cold 10µM EDTA with PBS with 5µg/mL of GNA-fluorescein. Samples were shielded from light and incubated on ice with GNA for 30 minutes. Following incubation, samples were washed three times and re-suspended to a volume of 50µl in 10µM EDTA PBS. Samples were then examined under a light microscope (Zeiss Axioskop 2, Zeiss, Jena, Germany) with 495nm wavelength excitation. Wild type CHO-S cells were used as a negative control and HEK 293 $GnTI^-$ were used as a positive control. Representative images were taken on a Leica DM5500 B Widefield Microscope (Leica Microsystems, Buffalo Grove, IL) at the UC Santa Cruz microscopy center.

Experimental protein production

An expression plasmid containing the gene encoding gp120 from the A244 strain of HIV (Genbank accession number: MG189369) was selected for transient transfection experiments. The protein encoded by this gene was identical to that used to produce the AIDSVAX B/E vaccine used in the RV144 trials (13, 14) with the exception that the N-linked glycosylation site at N334 was moved to N332. For analytical scale experiments, a total of $4x10^5$ cells from each candidate $MGAT1^-$ CHO line were placed in 450µl of media in a 24 well cell culture plate. Fugene, 1.7µL, (Promega, Madison, WI)

was pre-incubated at room temperature for 30 minutes with 550ng of DNA in a total volume of 50μL of media. Then 50μL of Fugene/DNA mixture was added to each well for a final transfected volume of 500μL. Aliquots of supernatant were removed for assay 72 hours post transfection.

For preparative scale transient transfection experiments, CHO cells were electroporated following the above MaxCyte method. Twenty-four hours post electroporation, the culture was supplemented with 1mM sodium butyrate (Thermo Fisher, Life Technologies, Carlsbad, CA) and temperature lowered to 32°C. The cultures were fed daily the equivalent of 3.5% of the original volume with Molecular Devices CHO A Feed (Molecular Devices, Sunnyvale, CA), 0.5% Yeastolate (BD, Franklin Lakes, NJ), 2.5% CHO-CD Efficient Feed A; and 0.25mM GlutaMax, 2 g/L Glucose (Sigma-Aldrich St. Louis, MO). Cultures were run until cell viability dropped below 50%. Supernatant was harvested by pelleting the cells at 250g for 30 minutes followed by pre-filtration through Nalgene™ Glass Pre-filters (Thermo Scientific, Waltham, MA) and 0.45 micron SFCA filtration (Nalgene, Thermo Scientific, Waltham, MA), then stored frozen at -20°C until purification. Proteins were purified using an N-terminal affinity tag derived from type 1 herpes simplex virus glycoprotein D (gD) as previously described (16).

Glycosidase digestion and SDS-PAGE

Endo H and PNGase F (New England BioLabs, Ipswich, MA) digests were performed per the manufacturer's protocol on 5ug of purified envelope protein using one unit of glycosidase. Samples were reduced and denatured then digested overnight at 37°C. Digested samples were run on NuPAGE (Thermo Fisher, Invitrogen, Carlsbad,

CA) 4-12% BisTris precast gels in MES running buffer then stained with SimplyBlue stain (Thermo Fisher, Invitrogen, Carlsbad, CA).

Fluorescence immunoassays to measure antibody binding

A fluorescence immunoassay (FIA) was used to measure the binding of polyclonal or monoclonal antibodies to recombinant envelope proteins. For antibody binding to purified proteins, Greiner Fluortrac 600 microtiter plates (Greiner Bio One, Kremsmünster, Austria) were coated with 2ug/mL of purified envelope protein overnight in PBS with shaking. Plates were blocked in PBS + 2.5% BSA (blocking buffer for 90 minutes, then washed four times with PBS containing 0.05% Tween-20 (Sigma). Serial dilutions of monoclonal antibodies were added in a range from 10ug/mL to 0.0001ug/mL, and then incubated at 25^{o}C for 90 minutes with shaking. After incubation and washing, 488 Alexa Fluor conjugated anti-human or anti-murine (Invitrogen, CA) was added at a 1:3000 dilution in PBS + 1% BSA. Plates were incubated for 90 minutes with shaking then washed four times with 0.05% Tween PBS using an automated plate washer. Plates were then imaged in a plate spectrophotometer (Envision System, Perkin Elmer) at excitation and emission wavelengths of 395nm and 490nm respectively. For antibody binding to unpurified envelope proteins in cell culture supernatants, Greiner Fluortrac 600 microtiter plates (Greiner Bio-one, Germany) were coated with 2ug/mL of purified mouse monoclonal antibody to an epitope in the V2 domain (10C10) or the gD purification tag (34.1) overnight in PBS with shaking. Plates were blocked in PBS + 2.5% BSA blocking buffer for 90 minutes, then washed four times with PBS containing 0.05% Tween-20 (Sigma). 150µl of 40x diluted supernatant were then added to each well or 10µg/mL of purified protein in control lanes, then

incubated at 25°C for 90minutes with shaking. After incubation and washing, PG9 was added in a range from 10μg/mL to 0.0001μg/mL, and then incubated at 25°C for 90minutes with shaking. After incubation and washing, fluorescently conjugated anti-human or anti-murine (Invitrogen, CA) was added at a 1:3000 dilution. Plates were incubated for 90 minutes with shaking then washed four times with 0.05% Tween PBS using an automated plate washer. Plates were then imaged in a plate spectrophotometer (Envision System, Perkin Elmer, Waltham, MA) at excitation and emission wavelengths of 395nm and 490nm respectively.

The broadly neutralizing monoclonal antibody PG9 was purchased from Polymun (Klosterneuburg, Austria) or produced in-house using 293 HEK cells from a synthetic gene created on the basis of published sequence data (available from the NIH AIDS Reagent Program, Germantown, MD). Alexa Fluor 488 conjugated anti-human IgG, anti-rabbit IgG, and anti-mouse IgG polyclonal antibodies were obtained from Invitrogen (Invitrogen, Thermo Fisher, Carlsbad, CA)

Glycan composition analysis by MALDI-TOF-MS

Glycoprotein sample (~100 μg) suspended in 50 mM ammonium bicarbonate buffer was incubated with trypsin (5μg, Sigma Aldrich), for 18 h at 37 °C. Digested peptides were desalted and purified by passing through a C18 sep-pak cartridge after inactivating trypsin by heating at 95 °C for 5 min. The purified peptides were then treated with PNGase F (23 IUB milliunits, NEB#P0705, New England BioLabs, Ipswich, MA) at 37 ˚C for 16 h, to release the N-glycans. The released N-glycans were desalted and purified from the peptides by C18 sep-pak cartridge followed by freeze-drying. Finally, the N-glycans were permethylated for 10 min at RT, by using 100 μl of methyl iodide in

682 the presence of NaOH/DMSO base (350 µl). The reaction was quenched by adding
683 water (1 ml) and the permethylated N-glycans were extracted by organic phase
684 separation using dichloromethane (2 ml). The excess of dichloromethane was removed
685 by stream of nitrogen and subsequently, prepared for MALDI-MS analysis (84).
686 Permethylated N-glycans were dissolved in methanol (20 µl) and small aliquot (~1 µl)
687 was spotted on to MALDI plate (Opti-TOF-384 well insert, Applied Biosystems, Foster
688 City, CA) and crystallized with DHB matrix (20 mg/ml in 50 % Methanol/water, Sigma
689 Aldrich). Data were obtained from AB SCIEX MALDI TOF/TOF 5800 (Applied
690 Biosystem MDS Analytical Technologies, Foster City, CA) mass spectrometer in
691 reflector positive-ion mode. Data analysis was performed by using Data Explorer V4.5,
692 and the assignment of glycan structure was based on the primary mass (m/z) coupled
693 with MS/MS fragmentation profile using the Expasy database online and the glycowork
694 bench software analysis (84, 85).

695 ## Minute Virus of Mice infectivity assay and sterility testing

696 IDEXX BioResearch (Columbia, MO) performed a Minute Virus of Mice (MVM)
697 infectivity assay. Cells were cultured at $4x10^5$ cells/mL, in 100mL total volume under
698 conditions described above in a spinner flask for five days. CHO-S and MGAT1$^-$ CHO
699 cells were infected with 1 multiplicity of infection (MOI) of MVM prototypic strain (MVMp)
700 or MVM Cutter strain (MVMc) and evaluated in triplicate. Five mL aliquots were
701 removed on days 1, 3, and 5, and cells were pelleted by centrifugation and stored at -
702 20°C. Day 5 samples were evaluated by quantitative polymerase chain reaction (qPCR)
703 for MVM and 18S using proprietary primers. The qPCR crossing point (CP) values were
704 reported and copy numbers based upon standard curves.

The cell line was tested for a panel of adventitious agents, cell line species, and in-vitro virus contamination by IDEXX BioResearch (Columbia, MO, USA) using a PCR based protocol described in supplemental materials.

Acknowledgments

Dr. Benjamin Abrams, UCSC Life Science Microscopy Center, provided technical support. Dr. Matthew H. Myles at IDEXX BioResearch developed and performed the MVM infectivity assays. Chelsea Didinger of the Department of Biomolecular Engineering at UCSC assisted with text and manuscript preparation.

References

1. Kwong PD, Wyatt R, Robinson J, Sweet RW, Sodroski J, Hendrickson WA. Structure of an HIV gp120 envelope glycoprotein in complex with the CD4 receptor and a neutralizing human antibody. Nature. 1998;393(6686):648-59.
2. Julien J-P, Cupo A, Sok D, Stanfield RL, Lyumkis D, Deller MC, et al. Crystal Structure of a Soluble Cleaved HIV-1 Envelope Trimer. Science. 2013;342(6165):1477-83.
3. McLellan JS, Pancera M, Carrico C, Gorman J, Julien JP, Khayat R, et al. Structure of HIV-1 gp120 V1/V2 domain with broadly neutralizing antibody PG9. Nature. 2011;480(7377):336-43.
4. Zhou T, Georgiev I, Wu X, Yang ZY, Dai K, Finzi A, et al. Structural basis for broad and potent neutralization of HIV-1 by antibody VRC01. Science. 2010;329(5993):811-7.
5. Ward AB, Wilson IA. Insights into the trimeric HIV-1 envelope glycoprotein structure. Trends in biochemical sciences. 2015;40(2):101-7.
6. Lavine CL, Lao S, Montefiori DC, Haynes BF, Sodroski JG, Yang X, et al. High-Mannose Glycan-Dependent Epitopes Are Frequently Targeted in Broad Neutralizing Antibody Responses during Human Immunodeficiency Virus Type 1 Infection. Journal of Virology. 2012;86(4):2153-64.
7. Horiya S, MacPherson IS, Krauss IJ. Recent strategies targeting HIV glycans in vaccine design. Nat Chem Biol. 2014;10(12):990-9.
8. Doores KJ, Burton DR. Variable Loop Glycan Dependency of the Broad and Potent HIV-1-Neutralizing Antibodies PG9 and PG16. Journal of Virology. 2010;84(20):10510-21.

738 9. Walker LM, Huber M, Doores KJ, Falkowska E, Pejchal R, Julien JP, et al. Broad
739 neutralization coverage of HIV by multiple highly potent antibodies. Nature.
740 2011;477(7365):466-70.
741 10. Kong L, Lee JH, Doores KJ, Murin CD, Julien JP, McBride R, et al. Supersite of
742 immune vulnerability on the glycosylated face of HIV-1 envelope glycoprotein gp120.
743 Nature structural & molecular biology. 2013;20(7):796-803.
744 11. Murin CD, Julien JP, Sok D, Stanfield RL, Khayat R, Cupo A, et al. Structure of
745 2G12 Fab2 in complex with soluble and fully glycosylated HIV-1 Env by negative-stain
746 single-particle electron microscopy. J Virol. 2014;88(17):10177-88.
747 12. Rerks-Ngarm S, Pitisuttithum P, Nitayaphan S, Kaewkungwal J, Chiu J, Paris
748 R, et al. Vaccination with ALVAC and AIDSVAX to Prevent HIV-1 Infection in Thailand.
749 New England Journal of Medicine. 2009;361(23):2209-20.
750 13. Berman PW. Development of bivalent rgp120 vaccines to prevent HIV type 1
751 infection. AIDS research and human retroviruses. 1998;14 Suppl 3:S277-89.
752 14. Berman PW, Huang W, Riddle L, Gray AM, Wrin T, Vennari J, et al.
753 Development of Bivalent (B/E) Vaccines Able to Neutralize CCR5-Dependent Viruses
754 from the United States and Thailand. Virology. 1999;265(1):1-9.
755 15. Paris RM, Kim JH, Robb ML, Michael NL. Prime–boost immunization with
756 poxvirus or adenovirus vectors as a strategy to develop a protective vaccine for HIV-1.
757 Expert Review of Vaccines. 2010;9(9):1055-69.
758 16. Yu B, Morales JF, O'Rourke SM, Tatsuno GP, Berman PW. Glycoform and Net
759 Charge Heterogeneity in gp120 Immunogens Used in HIV Vaccine Trials. PLoS ONE.
760 2012;7(8):e43903.
761 17. Geyer H, Holschbach C, Hunsmann G, Schneider J. Carbohydrates of human
762 immunodeficiency virus. Structures of oligosaccharides linked to the envelope
763 glycoprotein 120. Journal of Biological Chemistry. 1988;263(24):11760-7.
764 18. Doores KJ, Bonomelli C, Harvey DJ, Vasiljevic S, Dwek RA, Burton DR, et al.
765 Envelope glycans of immunodeficiency virions are almost entirely oligomannose
766 antigens. Proceedings of the National Academy of Sciences. 2010;107(31):13800-5.
767 19. Bonomelli C, Doores KJ, Dunlop DC, Thaney V, Dwek RA, Burton DR, et al. The
768 Glycan Shield of HIV Is Predominantly Oligomannose Independently of Production
769 System or Viral Clade. PLOS ONE. 2011;6(8):e23521.
770 20. Coss KP, Vasiljevic S, Pritchard LK, Krumm SA, Glaze M, Madzorera S, et al.
771 HIV-1 Glycan Density Drives the Persistence of the Mannose Patch within an Infected
772 Individual. Journal of Virology. 2016;90(24):11132-44.
773 21. Morales JF, Morin TJ, Yu B, Tatsuno GP, O'Rourke SM, Theolis R, et al. HIV-1
774 Envelope Proteins and V1/V2 Domain Scaffolds with Mannose-5 to Improve the
775 Magnitude and Quality of Protective Antibody Responses to HIV-1. The Journal of
776 biological chemistry. 2014;289(30):20526-42.
777 22. Lin Y-C, Boone M, Meuris L, Lemmens I, Van Roy N, Soete A, et al. Genome
778 dynamics of the human embryonic kidney 293 lineage in response to cell biology
779 manipulations. 2014;5:4767.
780 23. Stepanenko AA, Dmitrenko VV. HEK293 in cell biology and cancer research:
781 phenotype, karyotype, tumorigenicity, and stress-induced genome-phenotype evolution.
782 Gene. 2015;569(2):182-90.

783 24. Kim JY, Kim Y-G, Lee GM. CHO cells in biotechnology for production of
784 recombinant proteins: current state and further potential. Applied microbiology and
785 biotechnology. 2012;93(3):917-30.
786 25. Kunert R, Reinhart D. Advances in recombinant antibody manufacturing. Applied
787 microbiology and biotechnology. 2016;100:3451-61.
788 26. Möller J, Pörtner R. Model-Based Design of Process Strategies for Cell Culture
789 Bioprocesses: State of the Art and New Perspectives. In: Gowder SJT, editor. New
790 Insights into Cell Culture Technology. Rijeka: InTech; 2017. p. Ch. 05.
791 27. Bieberich E. Synthesis, processing, and function of N-glycans in N-glycoproteins.
792 Advances in neurobiology. 2014;9:47-70.
793 28. Moremen KW, Tiemeyer M, Nairn AV. Vertebrate protein glycosylation: diversity,
794 synthesis and function. Nature reviews Molecular cell biology. 2012;13(7):448-62.
795 29. Schwarz F, Aebi M. Mechanisms and principles of N-linked protein glycosylation.
796 Current opinion in structural biology. 2011;21(5):576-82.
797 30. Schachter H. The 'yellow brick road' to branched complex N-glycans.
798 Glycobiology. 1991;1(5):453-61.
799 31. Bork K, Horstkorte R, Weidemann W. Increasing the sialylation of therapeutic
800 glycoproteins: the potential of the sialic acid biosynthetic pathway. Journal of
801 pharmaceutical sciences. 2009;98(10):3499-508.
802 32. Berger M, Kaup M, Blanchard V. Protein Glycosylation and Its Impact on
803 Biotechnology. In: Hu WS, Zeng A-P, editors. Genomics and Systems Biology of
804 Mammalian Cell Culture. Berlin, Heidelberg: Springer Berlin Heidelberg; 2012. p. 165-
805 85.
806 33. Emr S, Glick BS, Linstedt AD, Lippincott-Schwartz J, Luini A, Malhotra V, et al.
807 Journeys through the Golgi--taking stock in a new era. The Journal of cell biology.
808 2009;187(4):449-53.
809 34. Llop E, Gutierrez-Gallego R, Segura J, Mallorqui J, Pascual JA. Structural
810 analysis of the glycosylation of gene-activated erythropoietin (epoetin delta, Dynepo).
811 Analytical biochemistry. 2008;383(2):243-54.
812 35. Cummings RD. The repertoire of glycan determinants in the human glycome.
813 Molecular bioSystems. 2009;5(10):1087-104.
814 36. Li H, d'Anjou M. Pharmacological significance of glycosylation in therapeutic
815 proteins. Current opinion in biotechnology. 2009;20(6):678-84.
816 37. Mizuochi T, Spellman MW, Larkin M, Solomon J, Basa LJ, Feizi T. Carbohydrate
817 structures of the human-immunodeficiency-virus (HIV) recombinant envelope
818 glycoprotein gp120 produced in Chinese-hamster ovary cells. The Biochemical journal.
819 1988;254(2):599-603.
820 38. Reitter JN, Means RE, Desrosiers RC. A role for carbohydrates in immune
821 evasion in AIDS. Nat Med. 1998;4(6):679-84.
822 39. Go EP, Hewawasam G, Liao HX, Chen H, Ping LH, Anderson JA, et al.
823 Characterization of glycosylation profiles of HIV-1 transmitted/founder envelopes by
824 mass spectrometry. J Virol. 2011;85(16):8270-84.
825 40. Cao L, Diedrich JK, Kulp DW, Pauthner M, He L, Park S-KR, et al. Global site-
826 specific N-glycosylation analysis of HIV envelope glycoprotein. 2017;8:14954.
827 41. Go EP, Herschhorn A, Gu C, Castillo-Menendez L, Zhang S, Mao Y, et al.
828 Comparative Analysis of the Glycosylation Profiles of Membrane-Anchored HIV-1

Envelope Glycoprotein Trimers and Soluble gp140. Journal of Virology. 2015;89(16):8245-57.
42. Gottlieb C, Skinner SAM, Kornfeld S. Isolation of a Clone of Chinese Hamster Ovary Cells Deficient in Plant Lectin-Binding Sites. Proceedings of the National Academy of Sciences. 1974;71(4):1078-82.
43. Stanley P, Narasimhan S, Siminovitch L, Schachter H. Chinese hamster ovary cells selected for resistance to the cytotoxicity of phytohemagglutinin are deficient in a UDP-N-acetylglucosamine--glycoprotein N-acetylglucosaminyltransferase activity. Proceedings of the National Academy of Sciences of the United States of America. 1975;72(9):3323-7.
44. Hsu Patrick D, Lander Eric S, Zhang F. Development and Applications of CRISPR-Cas9 for Genome Engineering. Cell.157(6):1262-78.
45. Sander JD, Joung JK. CRISPR-Cas systems for editing, regulating and targeting genomes. Nat Biotech. 2014;32(4):347-55.
46. GenBank [Internet]. 2016.
47. Binley JM, Ban Y-EA, Crooks ET, Eggink D, Osawa K, Schief WR, et al. Role of Complex Carbohydrates in Human Immunodeficiency Virus Type 1 Infection and Resistance to Antibody Neutralization. Journal of Virology. 2010;84(11):5637-55.
48. Kaku H, Goldstein IJ. [27] Snowdrop lectin. Methods in enzymology. 179: Academic Press; 1989. p. 327-31.
49. Zhu X, Borchers C, Bienstock RJ, Tomer KB. Mass Spectrometric Characterization of the Glycosylation Pattern of HIV-gp120 Expressed in CHO Cells. Biochemistry. 2000;39(37):11194-204.
50. Go EP, Liao H-X, Alam SM, Hua D, Haynes BF, Desaire H. Characterization of Host-Cell Line Specific Glycosylation Profiles of Early Transmitted/Founder HIV-1 gp120 Envelope Proteins. Journal of proteome research. 2013;12(3):1223-34.
51. Kwong PD, Mascola JR, Nabel GJ. Broadly neutralizing antibodies and the search for an HIV-1 vaccine: the end of the beginning. Nature Reviews Immunology. 2013;13:693.
52. Li Y, O'Dell S, Walker LM, Wu X, Guenaga J, Feng Y, et al. Mechanism of neutralization by the broadly neutralizing HIV-1 monoclonal antibody VRC01. J Virol. 2011;85(17):8954-67.
53. Moody M, Alves W, Varghese J, Khan F. Mouse Minute Virus (MMV) Contamination--A Case Study: Detection, Root Cause Determination, and Corrective Actions. PDA journal of pharmaceutical science and technology. 2011;65(6):580-8.
54. Nam HJ, Gurda-Whitaker B, Gan WY, Ilaria S, McKenna R, Mehta P, et al. Identification of the sialic acid structures recognized by minute virus of mice and the role of binding affinity in virulence adaptation. The Journal of biological chemistry. 2006;281(35):25670-7.
55. Halder S, Cotmore S, Heimburg-Molinaro J, Smith DF, Cummings RD, Chen X, et al. Profiling of Glycan Receptors for Minute Virus of Mice in Permissive Cell Lines Towards Understanding the Mechanism of Cell Recognition. PLOS ONE. 2014;9(1):e86909.
56. Huang L-Y, Halder S, Agbandje-McKenna M. Parvovirus Glycan Interactions. Current opinion in virology. 2014;0:108-18.

874 57. Garcin PO, Panté N. The minute virus of mice exploits different endocytic
875 pathways for cellular uptake. Virology. 2015;482:157-66.
876 58. Besselsen DG, Pintel DJ, Purdy GA, Besch-Williford CL, Franklin CL, Hook RR,
877 et al. Molecular characterization of newly recognized rodent parvoviruses. Journal of
878 General Virology. 1996;77(5):899-911.
879 59. Moore JP, McKeating JA, Jones IM, Stephens PE, Clements G, Thomson S, et
880 al. Characterization of recombinant gp120 and gp160 from HIV-1: binding to monoclonal
881 antibodies and soluble CD4. AIDS. 1990;4(4):307-16.
882 60. Jones DH, McBride BW, Roff MA, Farrar GH. Efficient purification and rigorous
883 characterisation of a recombinant gp120 for HIV vaccine studies. Vaccine.
884 1995;13(11):991-9.
885 61. Schnittman SM, Lane HC, Roth J, Burrows A, Folks TM, Kehrl JH, et al.
886 Characterization of GP120 binding to CD4 and an assay that measures ability of sera to
887 inhibit this binding. The Journal of Immunology. 1988;141(12):4181.
888 62. Li Y, Luo L, Rasool N, Kang CY. Glycosylation is necessary for the correct
889 folding of human immunodeficiency virus gp120 in CD4 binding. J Virol. 1993;67(1):584-
890 8.
891 63. Rizzuto CD, Wyatt R, Hernandez-Ramos N, Sun Y, Kwong PD, Hendrickson WA,
892 et al. A conserved HIV gp120 glycoprotein structure involved in chemokine receptor
893 binding. Science. 1998;280(5371):1949-53.
894 64. Pritchard LK, Vasiljevic S, Ozorowski G, Seabright GE, Cupo A, Ringe R, et al.
895 Structural Constraints Determine the Glycosylation of HIV-1 Envelope Trimers. Cell
896 reports. 2015;11(10):1604-13.
897 65. Wei X, Decker JM, Wang S, Hui H, Kappes JC, Wu X, et al. Antibody
898 neutralization and escape by HIV-1. Nature. 2003;422(6929):307-12.
899 66. Wang Z, Lorin C, Koutsoukos M, Franco D, Bayat B, Zhang Y, et al.
900 Comprehensive Characterization of Reference Standard Lots of HIV-1 Subtype C
901 Gp120 Proteins for Clinical Trials in Southern African Regions. Vaccines. 2016;4(2).
902 67. Zambonelli C, Dey AK, Hilt S, Stephenson S, Go EP, Clark DF, et al. Generation
903 and Characterization of a Bivalent HIV-1 Subtype C gp120 Protein Boost for Proof-of-
904 Concept HIV Vaccine Efficacy Trials in Southern Africa. PLOS ONE.
905 2016;11(7):e0157391.
906 68. Munro S. What can yeast tell us about N-linked glycosylation in the Golgi
907 apparatus? FEBS Letters. 2001;498(2–3):223-7.
908 69. Walski T, De Schutter K, Damme E, Smagghe G. Diversity and functions of
909 protein glycosylation in insects2017. 21-34 p.
910 70. Elbein AD, Solf R, Dorling PR, Vosbeck K. Swainsonine: an inhibitor of
911 glycoprotein processing. Proceedings of the National Academy of Sciences of the
912 United States of America. 1981;78(12):7393-7.
913 71. Chang VT, Crispin M, Aricescu AR, Harvey DJ, Nettleship JE, Fennelly JA, et al.
914 Glycoprotein structural genomics: solving the glycosylation problem. Structure (London,
915 England : 1993). 2007;15(3):267-73.
916 72. Tokunaga F, Hara K, Koide T. N-linked oligosaccharide processing, but not
917 association with calnexin/calreticulin is highly correlated with endoplasmic reticulum-
918 associated degradation of antithrombin Glu313-deleted mutant. Archives of
919 biochemistry and biophysics. 2003;411(2):235-42.

73. Helenius A, Aebi M. Roles of N-linked glycans in the endoplasmic reticulum. Annual review of biochemistry. 2004;73:1019-49.
74. Mast SW, Moremen KW. Family 47 alpha-mannosidases in N-glycan processing. Methods in enzymology. 2006;415:31-46.
75. Lederkremer GZ. Glycoprotein folding, quality control and ER-associated degradation. Current opinion in structural biology. 2009;19(5):515-23.
76. Sealover NR, Davis AM, Brooks JK, George HJ, Kayser KJ, Lin N. Engineering Chinese hamster ovary (CHO) cells for producing recombinant proteins with simple glycoforms by zinc-finger nuclease (ZFN)-mediated gene knockout of mannosyl (alpha-1,3-)-glycoprotein beta-1,2-N-acetylglucosaminyltransferase (Mgat1). J Biotechnol. 2013;167(1):24-32.
77. Puthalakath H, Burke J, Gleeson PA. Glycosylation defect in Lec1 Chinese hamster ovary mutant is due to a point mutation in N-acetylglucosaminyltransferase I gene. The Journal of biological chemistry. 1996;271(44):27818-22.
78. Stanley P. Chinese hamster ovary cell mutants with multiple glycosylation defects for production of glycoproteins with minimal carbohydrate heterogeneity. Molecular and cellular biology. 1989;9(2):377-83.
79. Kwong Peter D, Mascola John R. Human Antibodies that Neutralize HIV-1: Identification, Structures, and B Cell Ontogenies. Immunity.37(3):412-25.
80. Klein F, Mouquet H, Dosenovic P, Scheid JF, Scharf L, Nussenzweig MC. Antibodies in HIV-1 Vaccine Development and Therapy. Science. 2013;341(6151):1199-204.
81. Haynes BF, Kelsoe G, Harrison SC, Kepler TB. B-cell–lineage immunogen design in vaccine development with HIV-1 as a case study. Nature biotechnology. 2012;30:423.
82. Yu B, Fonseca DPAJ, O'Rourke SM, Berman PW. Protease Cleavage Sites in HIV-1 gp120 Recognized by Antigen Processing Enzymes Are Conserved and Located at Receptor Binding Sites. Journal of Virology. 2010;84(3):1513-26.
83. Coordinators NR. Database resources of the National Center for Biotechnology Information. Nucleic Acids Research. 2016;44(Database issue):D7-D19.
84. Shajahan A, Supekar NT, Heiss C, Ishihara M, Azadi P. Tool for Rapid Analysis of Glycopeptide by Permethylation via One-Pot Site Mapping and Glycan Analysis. Analytical chemistry. 2017;89(20):10734-43.
85. Sheikh MO, Thieker D, Chalmers G, Schafer CM, Ishihara M, Azadi P, et al. O2 sensing-associated glycosylation exposes the F-box-combining site of the Dictyostelium Skp1 subunit in E3 ubiquitin ligases. The Journal of biological chemistry. 2017;292(46):18897-915.

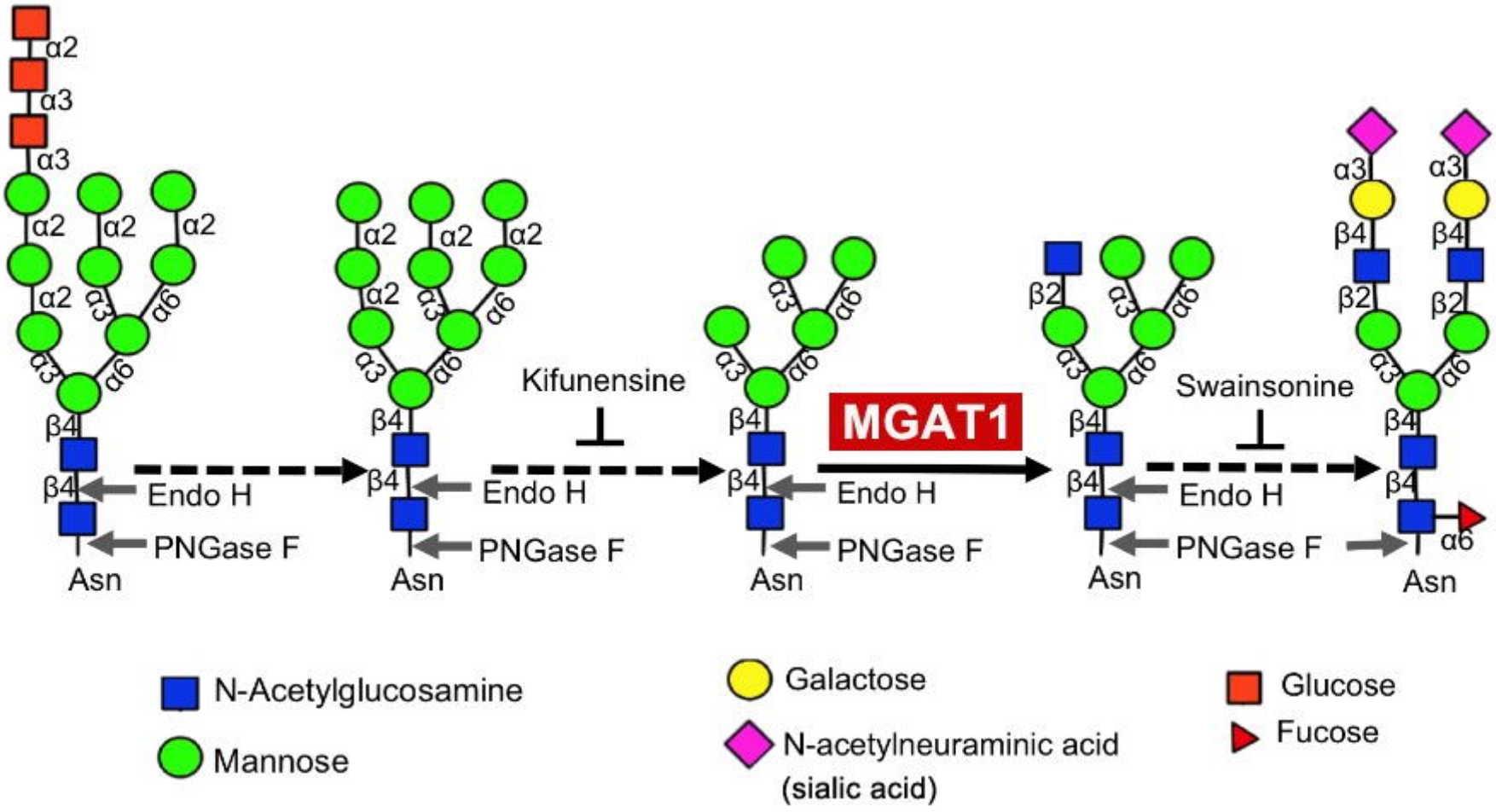
α2
α3
α3
α2
α2
α2
α2
α3
α6
β4
β4
Endo H
PNGase F
Asn
Kifunensine
MGAT1
Swainsonine
β2
N-Acetylglucosamine
Mannose
Galactose
N-acetylneuraminic acid
(sialic acid)
Glucose
Fucose

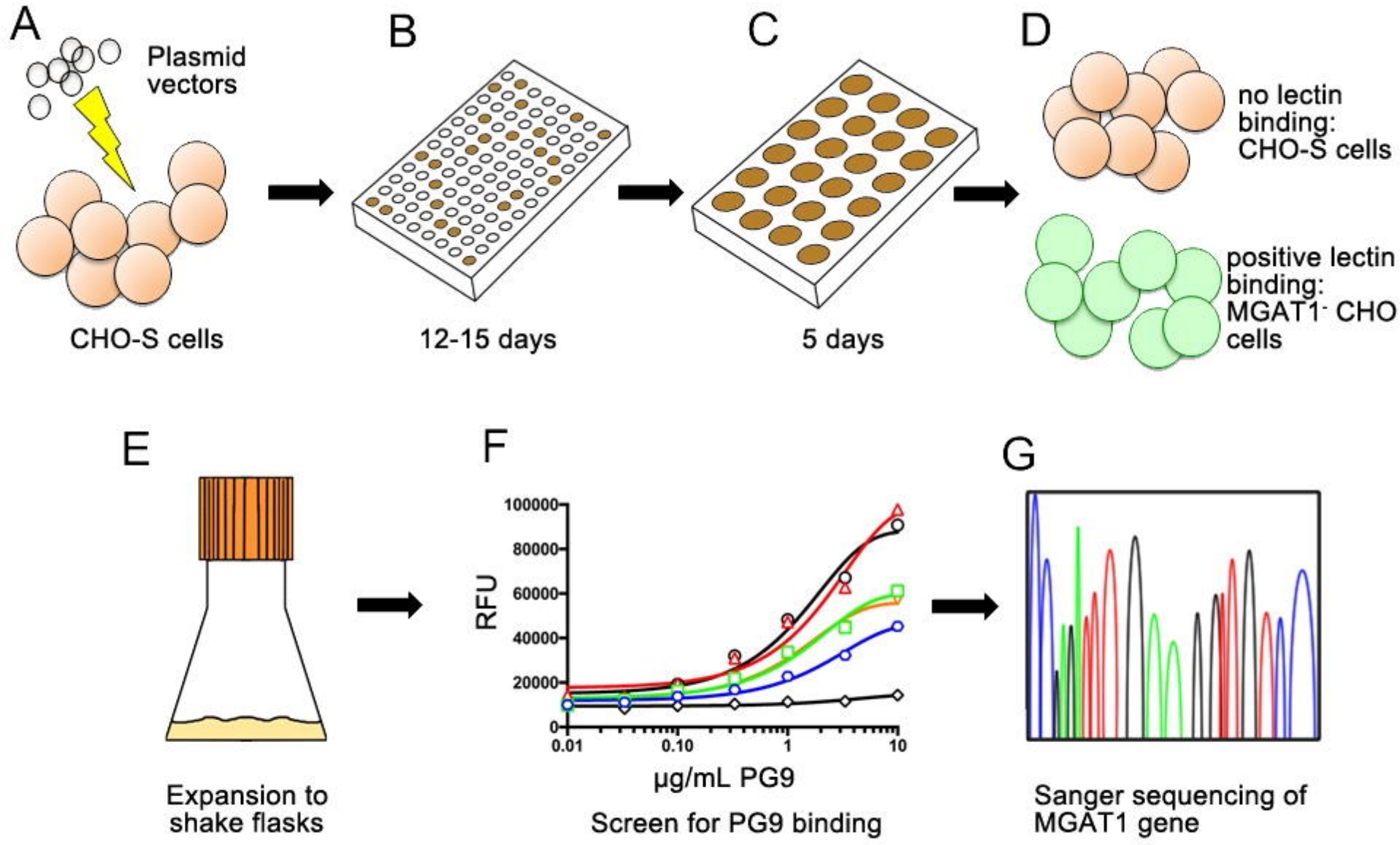
A
Plasmid vectors
CHO-S cells
B
12-15 days
C
5 days
D
no lectin binding: CHO-S cells
positive lectin binding: MGAT1- CHO cells
E
Expansion to shake flasks
F
RFU
100000
80000
60000
40000
20000
0
0.01
0.10
1
10
µg/mL PG9
Screen for PG9 binding
G
Sanger sequencing of MGAT1 gene

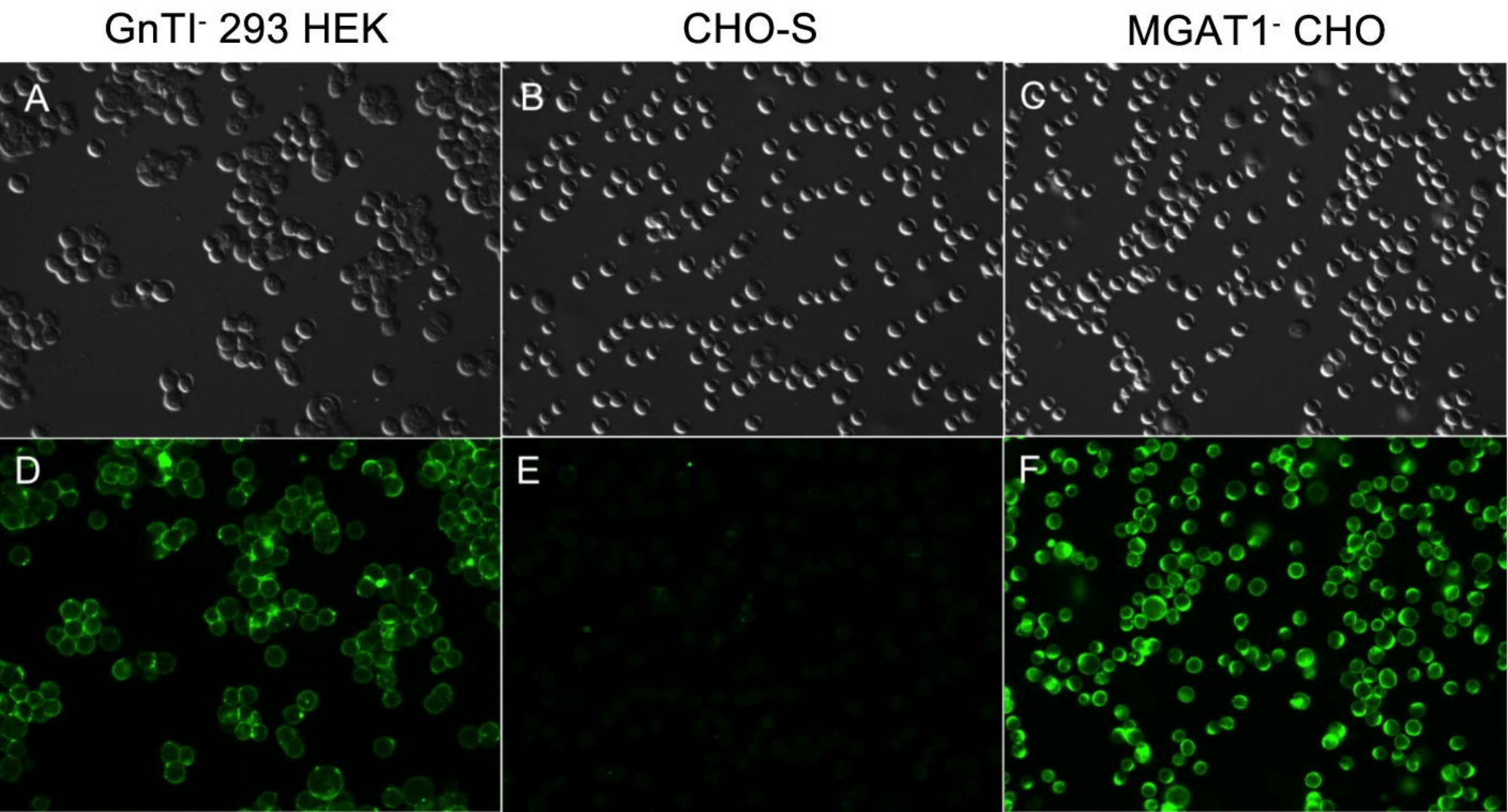
GnTI- 293 HEK
CHO-S
MGAT1- CHO
A
B
C
D
E
F

A

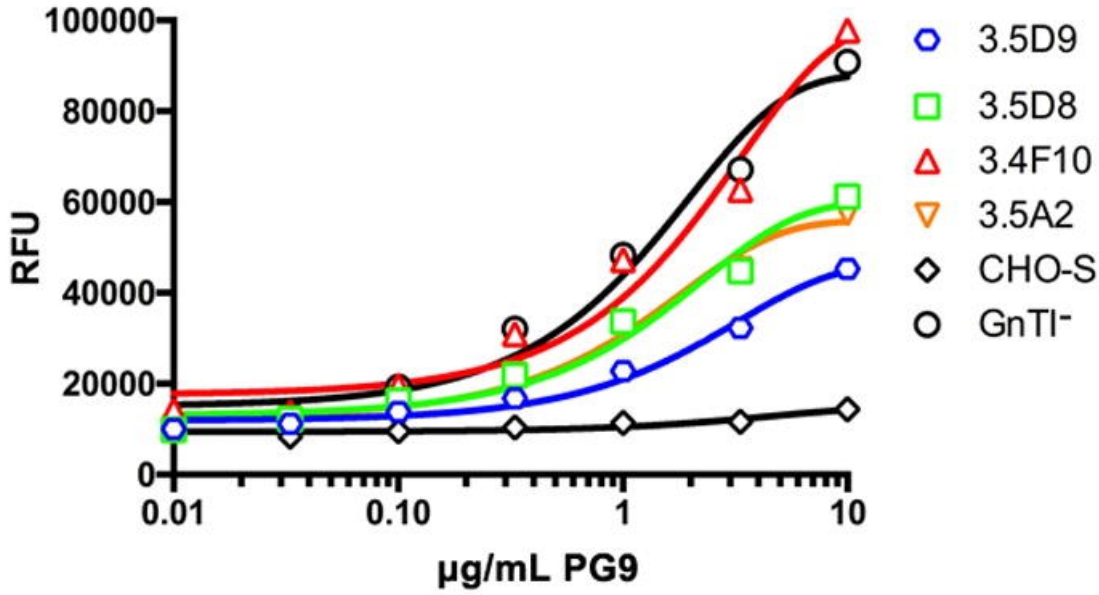

B

CHO-S

5'-TGCTTTGGGGTGCTATCCTCTTTGTGGGCTGGAATGCCCT-3'
3'-ACGAAACCCCACGATAGGAGAAACACCCCACCTTACGGGA-5'

PAM gRNA complement

C

3.4F10 & 3.5D8

5'-TGCTTTGGGGTGCTATCCTCTTTTGTGGGCTGGAATGCCCT-3'
3'-ACGAAACCCCACGATAGGAGAAAACACCCCACCTTACGGGA-5'

single base added

D

3.5A2

5'-TGCTTTGGGGTGCTATCCTCTTTGTGGGCTGGAATGCCCT-3'
3'-ACGAAACCCCACGATAGGAGAAACACCCCACCTTACGGGA-5'

30 bases deleted

E

3.5D9

5'-TGCTTTGGGGTGCTATCCTCTTTGTGGGCTGGAATGCCCT-3'
3'-ACGAAACCCCACGATAGGAGAAACACCCCACCTTACGGGA-5'

24 bases deleted

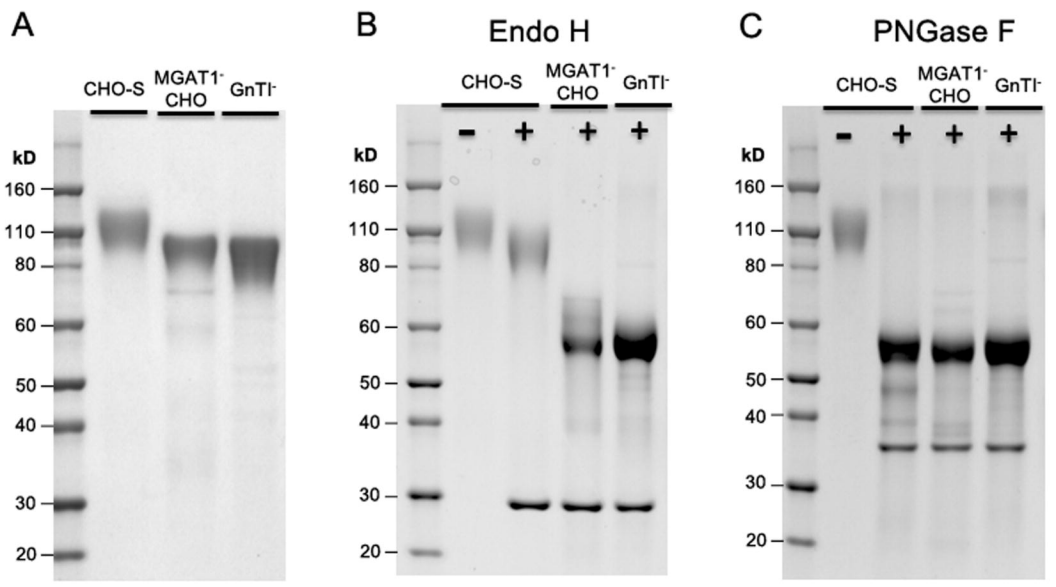
A
CHO-S
MGAT1- CHO
GnTI-
kD
160
110
80
60
50
40
30
20
B
Endo H
CHO-S
MGAT1- CHO
GnTI-
- + + +
kD
160
110
80
60
50
40
30
20
C
PNGase F
CHO-S
MGAT1- CHO
GnTI-
- + + +
kD
160
110
80
60
50
40
30
20

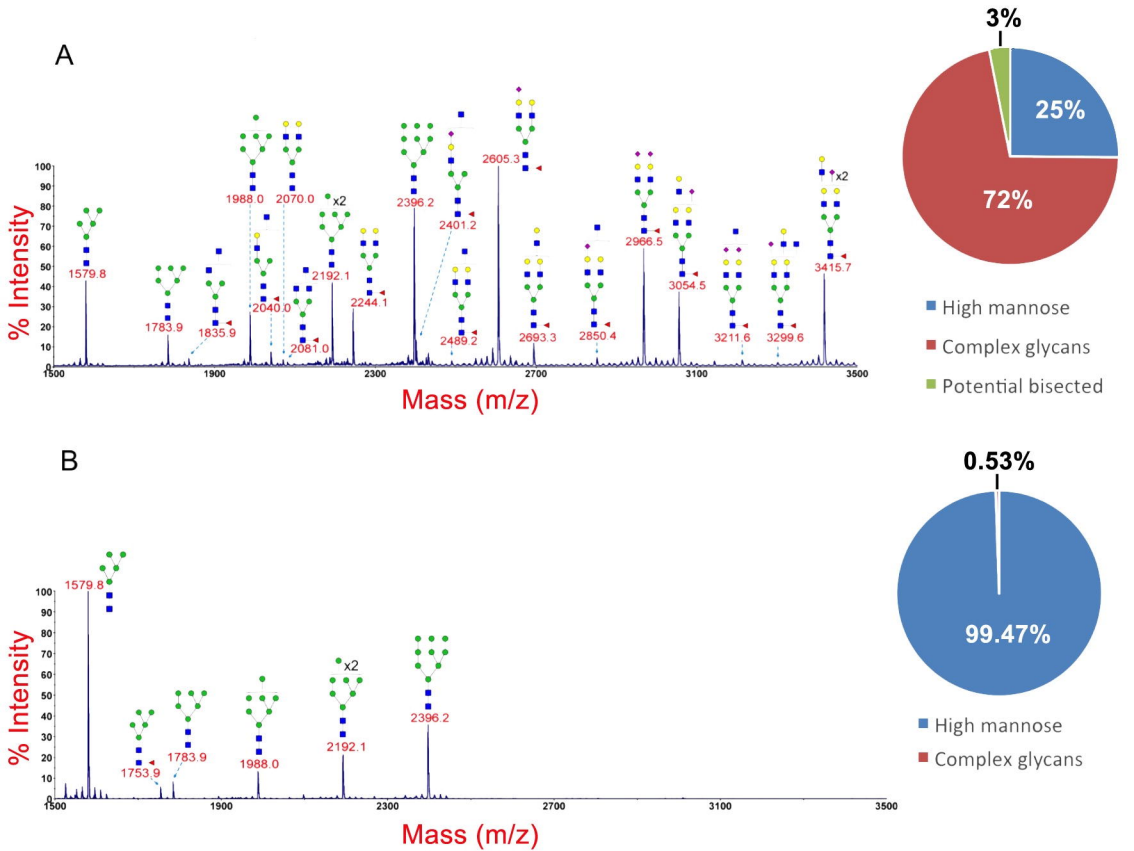
A
% Intensity
Mass (m/z)
1579.8
1783.9
1835.9
1988.0
2040.0
2070.0
x2
2081.0
2192.1
2244.1
2396.2
2401.2
2489.2
2605.3
2693.3
2850.4
2966.5
3054.5
3211.6
3299.6
3415.7
x2
3%
25%
72%
High mannose
Complex glycans
Potential bisected
B
% Intensity
Mass (m/z)
1579.8
1753.9
1783.9
1988.0
2192.1
x2
2396.2
0.53%
99.47%
High mannose
Complex glycans

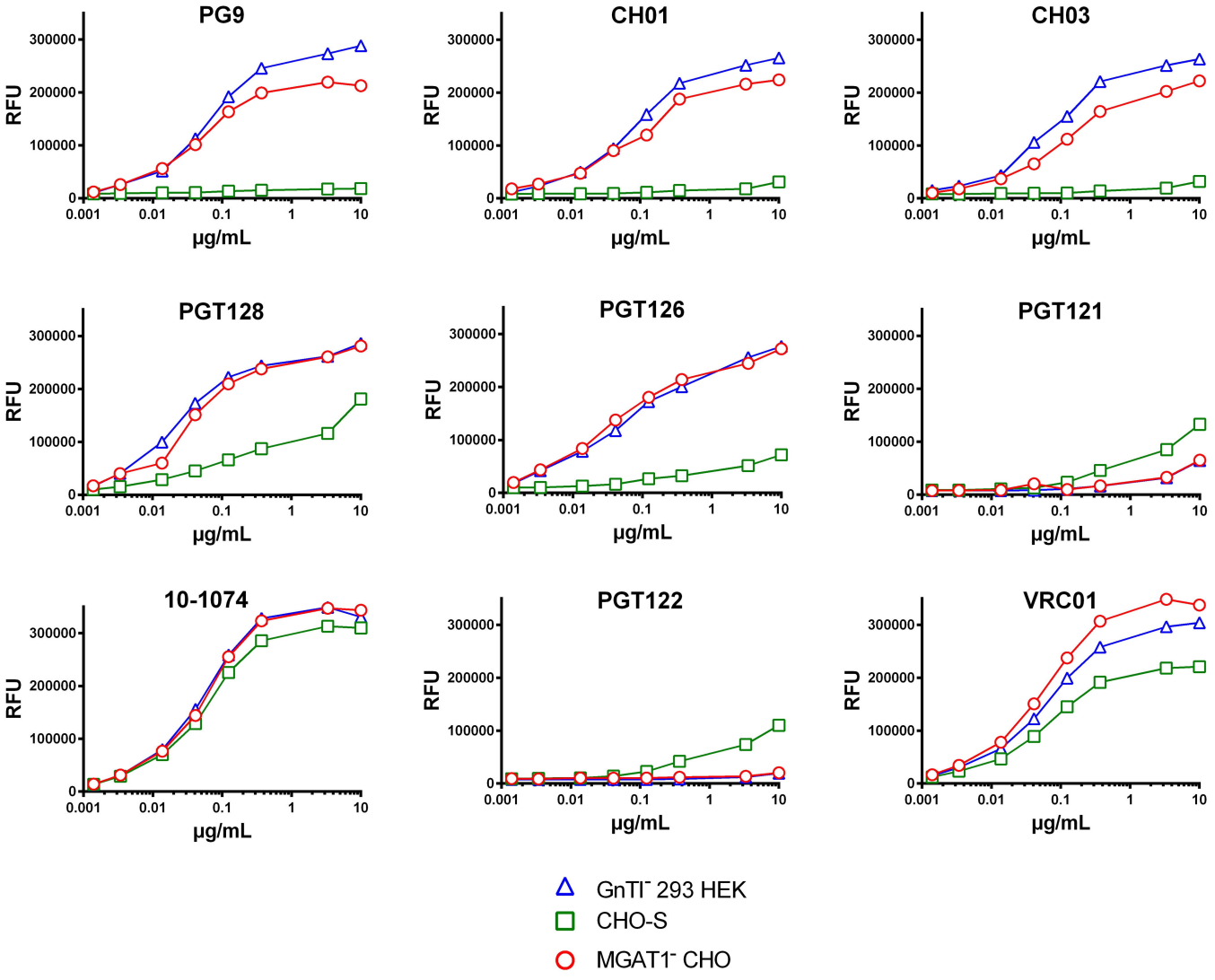
PG9
CH01
CH03
PGT128
PGT126
PGT121
10-1074
PGT122
VRC01
RFU
300000
200000
100000
0
0.001
0.01
0.1
1
10
µg/mL
GnTI⁻ 293 HEK
CHO-S
MGAT1⁻ CHO